

Mathematical Methods for Cylindrical Cellular Structures with Spatial Gradients in Membrane Capacitance

Jeff R. Knisley, Ph.D.¹ and Loyd Lee Glenn, Ph.D.²

¹Department of Mathematics, ^{1,2}Institute for Quantitative Biology, and

²Department of Mental Health of the College of Nursing

East Tennessee State University

Johnson City, TN 37614-1703

Running head: Non Uniform Membrane Capacitance

Keywords: cable equation, equivalent cylinder, membrane time constant, postsynaptic propagation, dendrite, transient response, ionophores, lipid bilayer

Please send correspondence and proofs to: Prof. L.L. Glenn, Department of Mental Health, College of Nursing, East Tennessee State University, Box 70403, Johnson City, TN 37614-1703. Phone: (423) 439-4067, Fax: (423) 439-4060, Email: glennl@etsu.edu

Abstract

A method based on complex residue theory was used to develop three mathematical models of cylindrical cell structures with non uniform membrane capacitance. The first model incorporated a membrane capacitance change at a single longitudinal point along the cylinder axis. The second model incorporated a step change in capacitance, so that two parts of the cylinder are of different capacitances. The third model incorporated an exponential distribution of capacitance. The stimulus-response properties of the models were compared under different configurations and fit to experimental data from dendritic neurons (spinal motoneurons). The exponential model had the best fit and most stable properties. Using this model, the key question was addressed of whether the amount of variation of membrane capacitance measured in experimental studies is sufficient to markedly alter the essential process of response to transient stimuli and passive propagation. We concluded that the levels of capacitance variation measured in cells does not alter electrical responses at levels that are physiologically significant and so the widespread assumption of uniform membrane capacitance is likely to be valid.

Introduction

Mathematical methods are often the only resort when an important problem is not amenable to known experimental or empirical methods. In the present study, mathematical methods are used to develop a cellular model, which is subsequently applied to the question of the physiological significance of non uniform cell membrane capacitance. Cell membranes are key building blocks of all cells, and regardless of cell type, have the hallmark electrical property of a constant capacitance near $1 \mu\text{F per cm}^2$ (Jameison and others 2003; Lewis 2000; Roth and Hauser 2001; Trevelyan and others 2002; Cole, 1968). The existence of an electrical capacitance across cell membranes is not superfluous, but instead, is vital to cell life (McCance and Huether 2001; Porth, 1998). Capacitance is used as a mechanism for rapid biological signaling and for integration of electrical signals over time and space. Capacitance-dependent synaptic integration is the basis of central nervous system function. Given its universal importance, alterations in membrane capacitance are a factor in the pathogenesis of a wide variety of disorders of importance in nursing, such as asbestos toxicity (Dopp and others 2000), seizures (Amzica and Neckelmann 1999), metal poisoning (Chanturiya and Nikoloshina 1994), and hearing loss (Santos-Sacchi and Navarrete 2002.)

Until recently, models of cellular integration have assumed a constant membrane capacitance over the cell, usually of $1 \mu\text{F/cm}^2$. Although there is wide agreement that cell membranes have an average membrane capacitance near $1 \mu\text{F per cm}^2$, recent experimental work has led to questions about the assumption that membrane capacitance is constant over the surface of a cell (Thurbon and others 1998). Membrane capacitance is dependent on ion channel density (Benzanilla and others

1991; Kilic and Lindau 2001; Schmid and others 2004; but see Gentet and others 2000), and evidence has been mounting that ion channels are often distributed unevenly in cells (Ramcharan and Matthews 1996; Fu and others 1996; Miles and others 1996; De Schutter and Bower 1994; Starr and Wolpaw 1994). The consequences of capacitative non uniformities in the passive propagation of electrical potentials in cylindrical membrane processes (such as axons, dendrites, and muscle fibers) are not known. In fact, the simplifying assumption that membrane capacitance is fixed has been made in almost all analytic and computational models of neurons and other cells to date (see reviews by Rall 1977; Lindsay and others 1999; Glenn and Knisley 2005).

No systematic studies have been conducted to test this assumption, so the present study was conducted to determine the effect of the simplifying assumption of spatially-constant membrane capacitance in electrical signal diffusion and propagation. Specifically, the electrical responses of membrane cylinders with uniform capacitance to those in which capacitance was not uniform were compared in mathematical models, while controlling for the average capacitance. In addition, three types of non uniform capacitance were tested: (1) point change in capacitance, (2) step change in capacitance, and (3) exponentially graded capacitance. The hypothesis tested was that there are no biologically-significant differences between membrane cylinders with a homogenous membrane capacitance and those with a heterogenous membrane capacitance (point, stepped, or exponentially-graded), provided that the spatial variation in capacitance is within the range of that estimated in experimental studies.

Definition of the General Model

For a membrane cylinder with spatially-graded capacitance, the model satisfies the cable equation

$$\frac{\partial^2 V}{\partial X^2} - R_m C_m(X) \frac{\partial V}{\partial t} - V = 0, \quad 0 < X < L \quad (1)$$

where $V(X, t)$ is membrane potential, R_m is the specific membrane resistance in ohms, C_m is the specific membrane capacitance in farads, L is the electrotonic length of the equivalent cylinder, and X is the electronic distance from the origin (in dimensionless units of the length constant, λ). Note that C_m is a function of X and varies with distance from origin, which is the end of the cylinder. We assume sealed-end boundary conditions

$$\frac{\partial V}{\partial X}(L, t) = 0 \quad (2)$$

$$\frac{\partial V}{\partial X}(0, t) = 0 \quad (3)$$

and also that the cell is initially saturated to steady state by a current stimulus of magnitude I^{stim} . Separation of variables $V(X, t) = \phi(X)T(t)$ yields

$$\phi'' + (\alpha R_m C_m(X) - 1)\phi = 0 \quad (4)$$

and

$$T' = -\alpha T \quad (5)$$

The solution is of the form (see Major and others 1994; Majors and Evans 1994; Glenn and Knisley 1999, 2005),

$$V(X, t) = \sum_{n=0}^{\infty} A_n \phi_n(X) e^{-\alpha_n t} \quad (6)$$

where the $\alpha_n > 0$ are the eigenvalues, the C_n are the Fourier coefficients and the ϕ_n are the separated solutions or eigenfunctions of Equations 1 - 3. We normalize the eigenfunctions so that $\phi_n(0) = 1$. At the proximal end of the cylinder,

$$V(0, t) = \sum_{n=0}^{\infty} A_n e^{-\alpha_n t}$$

On $L^2[0, L]$, we define the inner product

$$\langle f, g \rangle = \int_0^L f(X) g(X) \tau(X) dX$$

From Sturm-Liouville theory (Stackgold 1979) we have

$$\langle \phi_k, \phi_n \rangle = 0$$

if $n \neq k$, and that

$$A_n e^{-\alpha_n t} = \frac{\langle V(X, t), \phi_n \rangle}{\langle \phi_n, \phi_n \rangle} \quad (7)$$

which can be used to estimate the A_n once the eigenvalues and eigenfunctions are known. The Fourier coefficients can also be estimated using the method of residues, as shown below.

The initial potential distribution is the steady state distribution V^{ss} which satisfies

$$\frac{d^2 V^{ss}}{dX^2} - V^{ss} = 0, \quad 0 < X < L \quad (8)$$

$$\frac{dV^{ss}}{dX}(L) = 0 \quad (9)$$

$$\frac{dV^{ss}}{dX}(0) = I^{stim} \quad (10)$$

The solution is given by

$$V^{ss}(X) = \frac{-I^{stim} \cosh(L - X)}{G^\infty \sinh(L)} \quad (11)$$

where G^∞ is the input conductance. It follows that Equation 7 reduces to

$$A_n = \frac{\langle V^{ss}, \phi_n \rangle}{\langle \phi_n, \phi_n \rangle}$$

This approach was used to solve for three models of non uniform capacitance: (1) point change in capacitance, (2) step change in capacitance, and (3) exponentially graded capacitance.

Definition of Point and Stepped Models

If $C_m = C_m(L)$ and $C = C_m(0)$,

$$C_m(X) = \begin{cases} C & \text{if } 0 \leq X \leq Z \\ C_m & \text{if } Z < X \leq L \end{cases}$$

for any Z between 0 and L . By previous methods (Bluman and Tuckwell 1987, see appendices in Major and Evans 1994; Major and others 1993, 1994), the Laplace transform of the transient at $X = 0$ is

$$W(0) = \frac{I^{stim} b_s + b_m \tanh(b_s Z) \tanh(b_m(L-Z))}{G^\infty b_s b_m \tanh(b_m(L-Z)) + b_s \tanh(b_s L)} \quad (12)$$

where $b_s = \sqrt{sR_m C + 1}$ and $b_m = \sqrt{sR_m C_m + 1}$. If we assume that $\rho = G^\infty \tanh(L)/Z$ is constant with respect to Z , then Equation 12 is given by

$$W(0) = \frac{I^{stim} b_s + b_m \tanh(b_s Z) \tanh(b_m(L-Z))}{b_s G^\infty b_m \tanh(b_m(L-Z)) + \rho b_s \tanh(b_s Z) \coth(L)/Z}$$

We now show that the point membrane capacity model in Equation 12 is a limiting case of the varying capacity model when $C_m(X)$ is the step function. In the

limit as $Z \rightarrow 0$, the transient becomes

$$W(0) = \frac{I^{in}}{G^\infty \sqrt{sR_m C_m + 1} \tanh(\sqrt{sR_m C_m + 1}L) + \rho \coth(L)(sR_m C + 1)} \quad (13)$$

which is the solution for the voltage for a membrane cylinder with a different point membrane capacity at the origin.

Definition of an Exponentially-Graded Model

Models in which membrane capacitance changes are at a point or are stepped, have a discontinuity at the point of change that may not be biologically realistic. An exponentially graded model, on the other hand, has a smooth, continuous change in membrane capacitance, and thus might be more biologically realistic. The cable equation (Equation 1) cannot be solved in general. The same waveform can be well-approximated by more than one multi-exponential (Major and Evans 1994), so numerical solutions to Equations 1 - 3 are limited in their applicability to the problem of parameter identification. There are certain choices for $C_m(X)$ for which closed form solutions are possible, but for such choices of $C_m(X)$, it has not been possible to find closed form solutions for the eigenvalues and Fourier coefficients except in special cases. However, many choices for $C_m(X)$ lead to closed form expressions for the Laplace transform of the solution. From the Laplace transform solutions, the eigenvalues and Fourier coefficients can be determined using the theory of residues from complex analysis (Lanzcos 1961; Zauderer 1983; Wunsch 1994).

In particular, such a solution is possible if $C_m(X)$ represents the exponentially graded membrane capacitance given by

$$C_m(X) = \frac{\mu}{(1 + Me^{-2X})^2}$$

where for the ratio parameter $\varepsilon = C/C_m$ we have

$$M = \frac{1 - \sqrt{\varepsilon}}{\sqrt{\varepsilon} - e^{-2L}}$$

$$\mu = C(1 + M)^2$$

In Fig. 1, the relation between τ and L is shown for $\varepsilon = 0.9$, $R_m C_m = 0.005$. Notice how for cylinders with an electrotonic length greater than one, and a 10% exponential gradient in capacitance produces a decay time that is very close to that of the uniform capacitance model (in which $\tau = 0.005$ ms).

The Laplace transform of

$$\hat{V}'' - (sRC(X) + 1)\hat{V} = -C_m(X)V^{ss} \quad (14)$$

has a solution of the form

$$\hat{V}(X) = W(X) - \frac{V^{ss}(X)}{s},$$

where the transient W satisfies the homogeneous equation associated with Equation

14. The Laplace transform of the transient is given by

$$W(X) = \sqrt{Me^{-2x} + 1} \left(D_1 (M + e^{2x})^{\sqrt{s\mu+1/2}} + D_2 (M + e^{2x})^{-\sqrt{s\mu+1/2}} \right)$$

as can be verified by substitution. The sealed end boundary condition at $X = L$ yields

$$D_2 = D_1 \frac{\left(\sqrt{s\mu+1} - Me^{-2L} \right)}{\left(\sqrt{s\mu+1} + Me^{-2L} \right)} \left(M + e^{2L} \right)^{\sqrt{s\mu+1}}$$

which is combined with the other boundary condition to yield a transient at $X = 0$ of

$$W(0) = \frac{I^{stim} (M + 1)}{G^\infty s \left(\sqrt{s\mu+1} + M \right)} \frac{\left(\frac{M+1}{M+e^{2L}} \right)^{\sqrt{s\mu+1}} + \frac{\left(\sqrt{s\mu+1} - Me^{-2L} \right)}{\left(\sqrt{s\mu+1} + Me^{-2L} \right)}}{\left(\frac{\sqrt{s\mu+1} - M}{\sqrt{s\mu+1} + M} \right) \left(\frac{M+1}{M+e^{2L}} \right)^{\sqrt{s\mu+1}} - \frac{\left(\sqrt{s\mu+1} - Me^{-2L} \right)}{\left(\sqrt{s\mu+1} + Me^{-2L} \right)}} \quad (15)$$

Since the eigenvalues of Equation 5 are negative, the exponents in Equation 15 are imaginary, complex exponentials and De Moivre's formula, transform Equation 15 into the eigenvalue equation

$$\frac{\sqrt{\alpha R_m C_m - 1} + M \tan \left(\sqrt{\alpha R_m C_m - 1} \ln \left(\sqrt{M + 1} \right) \right)}{\sqrt{\alpha R_m C_m - 1} \tan \left(\sqrt{\alpha R_m C_m - 1} \ln \left(\sqrt{M + 1} \right) \right) - M} = \frac{\sqrt{\alpha R_m C_m - 1} + Me^{2L} \tan \left(\sqrt{\alpha R_m C_m - 1} \ln \left(\sqrt{M + e^{-2L}} \right) \right)}{\sqrt{\alpha R_m C_m - 1} \tan \left(\sqrt{\alpha R_m C_m - 1} \ln \left(\sqrt{M + e^{-2L}} \right) \right) - Me^{2L}}, \quad (16)$$

When M is chosen such that $\sqrt{\alpha_n \mu - 1} \neq M$, the coefficients A_n are of the form

$$A_n = \frac{-2I^{stim}(M+1)}{G^\infty \alpha_n \mu (\sqrt{\alpha_n \mu - 1} - M) f(\alpha_n)} \left(\cos \left(\sqrt{\alpha_n \mu - 1} \ln \left(\frac{M+1}{M+e^{2L}} \right) \right) \right. \quad (17)$$

$$\left. + i \sin \left(\sqrt{\alpha_n \mu - 1} \ln \left(\frac{M+1}{M+e^{2L}} \right) \right) + \left(\frac{i\sqrt{\alpha_n \mu - 1} - Me^{-2L}}{i\sqrt{\alpha_n \mu - 1} + Me^{-2L}} \right) \right)$$

where $f(\alpha_n)$ is given by

$$f(\alpha_n) = \frac{\cos \left(\sqrt{\alpha_n \mu - 1} \ln \left(\frac{M+1}{M+e^{2L}} \right) \right) + i \sin \left(\sqrt{\alpha_n \mu - 1} \ln \left(\frac{M+1}{M+e^{2L}} \right) \right)}{i\sqrt{\alpha_n \mu - 1}} \ln \frac{M+1}{M+e^{2L}}$$

$$- \frac{2M}{i\sqrt{\alpha_n \mu - 1}} \frac{(M^2 e^{-2L} - \alpha_n \mu + 1)(1 - e^{-2L})}{(i\sqrt{\alpha_n \mu - 1} - M)^2 (i\sqrt{\alpha_n \mu - 1} + Me^{-2L})^2}$$

The Fourier coefficients can also be obtained from the eigenvalue equation by the eigenslope method (Equation 16). The analytic solution for exponentially-graded membrane capacitance was thus obtained. Next, the properties of the point, stepped, and exponential models were compared.

Comparison Between Models With Non Uniform C_m

The four models (constant, point, step, and exponential) were compared to each

other and also to experimental data on neurons. For the comparison, we normalized the Fourier coefficients to the steady state, and calculated the exponential components that comprise the voltage decay response to stimulation at $X = 0$ ($\tau_0 = 1/\alpha_0$, $\tau_1 = 1/\alpha_1$, A_0 and A_1) for a model in which there was a step change in membrane capacitance at an arbitrary electrotonic distances, Z , from the origin (from Equation 16).

Table 1 shows that the exponentially varying model and the step change model had similar time constants and similar amplitude coefficients for a wide range of model parameters, rather than only one set of values. In Table 2, the response components τ_0 and τ_1 differed between the exponential and point model regardless of the choice of ρ . The time constants of the responses of the point model only have a good fit to the exponential model when ρ and the electrotonic length L were unconstrained (allowed to vary concurrently and independently). A good fit was found under the limited condition that $\rho = 1.55$ and $L = 0.7065$ in the parameter series tested in Table 1. This is in marked contrast to the relation between the exponentially varying model and the step change model, which had good fits over most values in the range.

For model configurations in which the first two time constants for the voltage decay of the point capacitance model do match those of the exponentially varying model, the amplitude coefficients of the point capacitance model, computed using Equation 12, still do not match those of the exponentially-varying model. When $C = 0.9 \mu F$ and $C_m = 1.0 \mu F$, the ratio of A_0 to the initial value V_m at $t = 0$ is 0.9038 for the point model, whereas the same ratio for the exponential model is 0.7551. Also, the ratio of A_1 to V^{ss} is 0.08791 for the point model, compared to 0.1481 for the

exponential model. Table 2 shows that the step model has amplitude coefficients similar to the exponential model. In the point model, the first two Fourier coefficients account for 99% of the steady state, which means that the higher amplitude coefficients must necessarily be extremely small. However, in the both the exponential and step models (Table 2), the first two coefficients account for only 90% of the steady state. This evidence indicates that the point model is not a preferred model, and may not be a valid model.

The shape dependence of the decay waveforms for the point model differed from those of the exponential model, as can be seen by comparing the two graphs in Fig. 2. Note, qualitatively, how little the point model in B resembles the continuous model in A. The family of curves had a common point of intersection in the exponential model but not in the point (Fig. 2B). In the both models, the initial decay was faster if the capacitance was lower at $X=0$ than that when $X > 0$. In the exponential model, however, the final decay (after 0.010 s) was slower if the capacitance was lower at $X=0$. In the point model, the final decay rates converged, becoming dominated by a single exponential, $\tau = R_m C$. When the decay response of the point model and exponential model were superimposed (not shown), the curves could not be made to fit for any combination of parameters. The point model could never be made to closely approximate the exponential model (< 5% overall fit), even for small variations in the capacitance at the origin (i.e., C at $X=0$).

Comparison of Model Responses to Cells Responses

The next question addressed was whether a single membrane cylinder model

with sealed ends and a point or exponential distribution of C_m could account for the voltage response of single quasi-cylindrical cells to a current pulse. Experimental data from studies on spinal motoneurons (stimulation and response determined at $X = 0$) were used for this purpose. The values of C , R_m , C_m , and L were chosen from experimental work on spinal motoneurons (Glenn and others 1987; Fleshman and others 1988; Clements and Redman 1989; Gentet and others 2000; Maltenfort and Hamm 2004). The multiexponential decomposition algorithm described in Knisley and Glenn (1996) was used to estimate τ_0 , τ_1 , A_0 and A_1 for a representative experimental response data from a series of spinal motoneurons, taken from the study of Glenn and others (1987). Fig. 3 shows the results of a best fit procedure between the experimental voltage recording and the theoretical response in the exponential model, and Table 3 shows the first two eigenvalues and initial amplitudes for the two waveforms. The parameters for the best fit under the assumption that was $C_m = 1 \mu\text{F}$, $C = 0.34 \mu\text{F}$, $R_m = 7,000 \Omega$, $L = 1.55$ and $V^{ss} = 0.01266$. Voltage transients produced by constant current pulses in the soma of neurons more closely approximated the exponential model than a point or stepped model. In experimental waveforms analyzed, A_0 has varies from 34% to 75% of the steady state value and has only rarely come close to 90% of steady state. Thus, the point capacitance model could not account for experimentally-derived curves of electrotonic responses in spinal motoneurons. The stepped model could if $0.3 < Z < .7$, which is remarkably the condition under which the step model most closely approximates the exponential model.

Errors Produced by Assumption of Constant C_m

In the previous sections, the mathematical model was developed and shown to fit empirical data best if an exponential distribution of capacitance was used. The final issue that will be addressed is how the response of a membrane cylinder with constant C_m compares to a cylinder with an exponential gradient in C_m under the conditions that the average C_m is the same in both and the variation in C_m is within the range measured in recent studies.

As shown in the responses of Fig. 4 and in measurements of decay rate derived from those responses in Table 4, a 2% gradient in membrane capacitance causes about a 1.0% error in the time to decay to 90% of the initial value, a 0.5% error in time to 50% decay, and a 0.3% error in time to 90% decay. A 10% gradient causes about a 7% change in time to decay to 90% of the initial value, a 3.5% error in time to 50% decay, and a 2.4% error in time to 90% decay.

Discussion

The main hypothesis tested by the mathematical models was that biologically-significant differences between membrane cylinders with a homogenous membrane capacitance and those with a heterogenous membrane capacitance (point, stepped, or exponentially-graded) affect passive responses, provided that the variation in capacitance is in the range of that estimated in experimental studies. This hypothesis was rejected. An exponential spatial variation in membrane capacitance at experimentally measured levels 5% produces a difference of 1.5% in the time it takes the voltage response to a step stimulus (Table 4) to decay to 50% of its initial value, as

compared to the assumption of a uniform membrane capacitance. This is a relatively small difference. Moreover, although the evidence is limited (see discussion below), the most that the capacitance would appear to change with distance is closer to 2%. Therefore, for most models of cells with a non uniform distribution of sodium channels or other channels, we conclude that the assumption of uniform membrane capacitance is largely valid.

The property of capacitance stems from the close proximity of two electrically conducting structures surfaces with the space between them filled by a poorly conducting medium. The membrane that envelops cells basically consists of a thin lipid bilayer that incorporates proteins, many of which span the membrane. The membrane capacitance stems from conductive extracellular fluid being separated by the inner hydrophobic layer of the cell membrane, which forms the poorly conducting structure required for the property of capacitance. The capacitance of the membranes depends on the thickness of the membrane, the number of carbons in the lipid chain that comprises the membrane, the electrical properties of the nonpolar, electrically-insulating interior of the bilayer membrane (dielectric constant), the location and density of nonpolar residues of the proteins embedded in the membrane (Risbo and others, 1997; Pethig, 1979, Thurbon and others 1998), and the size and time course of ion channel gating currents.

Studies in spinal neurons, brain neurons, cell migration, cardiac muscle cells, egg fertilization, and others (Hice, 1988; Masukawa and others 1991; Siegel and others 1994; Korchev and others 2000; Schwab 2001; Williams and Stuart 2003;) have been in agreement that ion channels are not generally uniformly distributed over the surface

of cell membranes. The question is unsettled, however, of whether or not the membrane capacitance changes according to the density of ion channels in the membrane.

Thurbon and others (1998) suggested that non uniformities in membrane capacitance are caused by ion channel proteins. Ion channel proteins could theoretically alter membrane capacitance by changing both the thickness and dielectric constant of the membrane. However, Gentet and others (2000) found no major changes in membrane capacitance from $0.9 \mu\text{F per cm}^2$ in kidney cells were transfected with a plasmid that added glycine receptors to the membrane. On the other hand, both theoretical work (Schmid and others 2004) and experimental work (Benzanilla and others 1991; Kilic and Lindau, 2001) found membrane capacitance to be dependent on the density of sodium or potassium channels in squid axon and pituitary nerve terminals. In models of the squid giant axon, Schmid and others (2004) concluded that “The membrane capacity at rest exhibits a bell-shaped dependence on the ion channel density.” The changes in membrane capacitance are attributed to gating currents, which are minute currents in the channel proteins themselves, associated with conformation changes between the open and closed states. For the squid giant axon, the change in membrane capacitance due to sodium channel gating currents ranged up to $0.15 \mu\text{F per cm}^2$ (Fernandez and others 1982), which is a 15% difference. Kilic and Lindau (2001) found the maximum capacitance change around $0.10 \mu\text{F}$ in pituitary nerve endings, which is a 3% difference in pituitary capacitance, however the average was lower at $0.03 \mu\text{F}$, which is a 1% difference. Thus, although the evidence is very limited, the maximum possible capacitance change to due ion channels would appear to be 15%, and a more typical value would be between 1% and 5%.

Validation of the Exponential Model

The second finding of this study is that the exponential model is the most suitable of the three models for use in studying the effects of non uniform membrane capacitance and for interpreting experimental studies. It may be the simplest mathematical form of models that have a continuous capacity gradient. This is evidenced by the fact that is the first and only continuous gradient model that has been solved to date.

The exponential model showed the most stable parameter dependence in the sense the decay components (eigenfunctions and eigen values) that comprised the decay responses varied the most smoothly and predictably as the parameters were varied (see next section for more discussion about stability). The exponential model also provided the best fit to experimental data.

Limited Applicability of the Point Capacitance Model

The third finding of the present study is that the use of an increased or decreased capacitance at a particular point (an infinitely small point) is not a good model for continuously graded capacitance. Instead, models with either exponentially distributed or stepped changes in capacitance have important advantages, one of which is ability to fit experimental data and the other is the ability to use the models for parameter identification.

Although we could not find any previous cases in the literature where models with point capacitances were studied, there many cases in which point resistance

changes have been studied. The most common of these is the shunt soma model for neurons (Durand 1984; Majors and others 1993, Poznanski 1996; Maltenfort and Hamm 2004). Several investigations have shown that models with point resistance changes in membrane properties are both biologically unrealistic and have undesirable analytic properties (Glenn and Knisley 1999; White and others 1992; Fleshman and others 1988). The primary problem is that point changes are mathematically ill-posed. The ill-posed nature of the inverse problem for a point change is illustrated by how a miniscule changes in waveform geometry can be induced by a relatively large change in τ_s . This was also shown by White and others (1992) for point resistance changes in membrane cylinders.

In our opinion, point changes in membrane properties, including conductance and capacitance, mitigate many of the advantages of using mathematical models to analyze the structure and function of cells, and so, should be avoided. Several previous studies have made similar findings in regard to point conductance models (White and others 1992 ; Glenn and Knisley 1999), but models that incorporate point changes in conductance (such as a somatic shunt in neurons) continue to be used.

The point model be avoided, even in cases where the capacitance is varies markedly in a small area (such as that caused by sodium channels at nodes of Ranvier of axons or at the axon hillock in neurons). For such cases, if the exponential model is not suitable, the step model should be used with a small, but not infinitesimally small, Z . The step model approximated the point model if $Z < 0.2$ in the step model, and became identical point model as $Z \rightarrow 0$. Thus, it is generally recommended that $Z > 0.2$ when using the step model.

Conclusion

This study is the first to derive the solutions for an analytic mathematical model of membrane cylinders (such as tube- or fiber-shaped cells or cylindrical processes such as dendrites) with spatially-varying membrane capacitance. Solved models are provided for point, stepped, and exponential capacitance changes with longitudinal distance along a cylinder. Comparison of the passive voltage responses of the three models to impulse stimuli and curve fitting of the responses to experimental voltage responses curve data from neurons found the exponential model to be the preferred model. Variation in the membrane capacitance of the exponential model of 5%, which is range found experimentally by others previously, produced only a 1.5% change in the half-time of the responses to impulses. The conclusion is drawn that the widespread assumption of uniform membrane capacitance over the surface of a cells is valid, in the sense that the degree of non uniformity found in cells is unlikely to affect electrical stimulus responses, electrotonic lengths, and postsynaptic propagation.

Acknowledgements

Supported by National Institutes of Health Grant R01 RR08659.

References

- Amzica F, Neckelmann D. 1999. Membrane capacitance of cortical neurons and glia during sleep oscillations and spike-wave seizures. *J Neurophysiol.* 82:2731-46.
- Bezanilla F, Perozo E, and others. 1991. Molecular basis of gating charge immobilization in Shaker potassium channels. *Science* 254:679-83.
- Bluman GW, Tuckwell HC. 1987. Techniques for obtaining analytical solutions for Rall's model neuron. *J Neurosci Methods* 20:151-166.
- Chanturiya AN, Nikoloshina HV. 1994. Correlations between changes in membrane capacitance induced by changes in ionic environment and the conductance of channels incorporated into bilayer lipid membranes. *J Membr Biol.* 1994 137:71-7.
- Clements JD, Redman SJ 1989. Cable properties of cat spinal motoneurons measured by combining voltage clamp, current clamp, and intracellular staining. *J Physiol (London)* 409:63-87.
- Cole KS. 1968. *Membranes, Ions and Impulses.* University of California Press, Berkeley, CA.
- De Schutter E, Bower JM. 1994. An active membrane model of the cerebellar Purkinje cell. i. simulation of current clamps in slice. *J Neurophysiology*, 71:375-400.

- Dopp E, Jonas L, Nebe B, Budde A, Knippel E. 2000. Dielectric changes in membrane properties and cell interiors of human mesothelial cells in vitro after crocidolite asbestos exposure. *Environ Health Perspect* 108:153-8.
- Durand D. 1984. The somatic shunt model for neurons. *Biophys J*, 46:645-653.
- Fernandez JM, Bezanilla F, and others. 1982. Distribution and kinetics of membrane dielectric polarization. II. Frequency domain studies of gating currents. *J Gen Physiol* 79:41-67
- Fleshman JW, Segev I, and others. 1988. Electrotonic architecture of type-identified alpha motoneurons in the cat spinal cord. *J Neurophysiol*, 60:60-85.
- Fu YS, Tseng GF, and others. 1996. Extrinsic inhibitory innervation to rubral neurons in rat brain-stem slices. *Exp Neurology*, 137:142-150.
- Gentet LJ, Stuart GJ, and others. 2000. Direct measurement of specific membrane capacitance in neurons. *Biophys J* 2000 79:314-20.
- Glenn LL and Knisley JR 1997. Use of eigenslope to estimate Fourier coefficients for passive cable models of the neuron. *Neurosci Res Comm* 21:187-194.
- Glenn LL, Knisley JR. 1999. Voltage Transients in Multipolar Neurons With Tapering Dendrites, Ch. 6, In: *Mathematical Modeling in the Neurosciences: From Ionic Channels to Neural Networks*, Edited by R. R. Poznanski, Harwood Academic Publishers, New York.

Glenn LL, Knisley JR 2005. Transients in branching multipolar neurons with tapering dendrites and sodium channels. In *Modeling in the Neurosciences: From Biological Systems to Neuromimetic Robotics*, 2nd Edition. Edited by: K.Lindsay, R. Poznanski, J.Rosenberg and O. Sporns. Taylor and Francis, London.

Glenn LL, Samojia BG, and others. 1987. Electrotonic parameters of cat spinal alpha motoneurons evaluated with an equivalent cylinder model that incorporates non-uniform membrane resistivity. *Brain Res* 435:398-402.

Glenn LL, Whitney JF, and others. 1988. Method for stable intracellular recordings of alpha motoneurons during treadmill walking in awake, intact cats. *Brain Res* 439:396-401.

Hice RE, Moody WJ. 1988. Fertilization alters the spatial distribution and the density of voltage-dependent sodium current in the egg of the ascidian *Boltenia villosa*. *Dev Biol* 127:408-20.

Jamieson J, Boyd HD, and others. 2003. Simulations to derive membrane resistivity in three phenotypes of guinea pig sympathetic postganglionic neuron. *J Neurophysiol* 89:2430-2440.

Kilic G, Lindau M. 2001. Voltage-dependent membrane capacitance in rat pituitary nerve terminals due to gating currents. *Biophys J* 80:1220-1229.

Kincaid D, Cheney W. 1991. *Numerical Analysis. Mathematics of Scientific*

Computing. Brooks/Cole Publ. Co., Pacific Grove, CA.

Knisley JR, Glenn LL. 1996. A linear method for the curve fitting of multiexponentials.

J Neurosci Methods. 67:177-83.

Korchev YE, Negulyaev YA, and others. 2000. Functional localization of single active

ion channels on the surface of a living cell. Nat Cell Biol 2:616-9.

Lanzcos C. 1961. Applied analysis. Prentice Hall, Englewood Cliffs, NJ

Lewis SA. 2000. Everything you wanted to know about the bladder epithelium but

were afraid to ask. Am J Physiol Renal Physiol 278:F867-F874.

Lindsay K, Ogden J, and others. 1999. An introduction to the principles of neuronal

modeling. In: *Modern Techniques in Neuroscience Research*, (Eds. U.

Windhorst & H. Johansson), Springer-Verlag, Ch 8, 213-306.

Major G, Evans J.D, and others. 1993. Solutions for transients in arbitrarily branching

cables: I. voltage recording with a somatic shunt. Biophys. J., 65:423-449.

Major G, Evans JD. 1994. Solutions for transients in arbitrarily branching cables: Iv.

non uniform electrical parameters. Biophys J. 66:615-634.

Major G, Larkman AU, and others. 1994. Detailed passive cable models of whole-cell

recorded ca3 pyrimidal neurons in fat hippocampal slices. J Neurosci, 14:4613-

4638.

- Maltenfort MG, Hamm TM. 2004. Estimation of the electrical parameters of spinal motoneurons using impedance measurements. *J Neurophysiol* 92:1433-44.
- Masukawa LM, Hansen AJ, and others. 1991. Distribution of single-channel conductances in cultured rat hippocampal neurons. *Cell Mol Neurobiol* 11:231-243.
- McCance K and Huether S. 2001. *Pathophysiology*. 4th Ed., Mosby, St. Louis, Mo.
- Miles R, Toth K, and others. 1996. Differences between somatic and dendritic inhibition in the hippocampus. *Neuron* 16:815-823.
- Pethig R, ed. 1979. *Dielectric and electronic properties of biological materials*. Chichester:Wiley.
- Porth C. 1998. *Pathophysiology: concepts of altered health states*. 5th Ed. Philadelphia: Lippincott.
- Poznanski RR. 1996. Transient response in a tapering cable model with somatic shunt. *NeuroReport* 7:1700-1704.
- Rall W. 1977. Core conductor theory and cable properties of neurons. In: *Handbook of Physiology. The Nervous System II*, Ed. by J. Brookhart and V.B. Mountcastle. Chap. 5, pages 39-97. Amer. Physiol. Soc., Bethesda, MD.
- Ramcharan EJ, Matthews MR.. 1996. Autoradiographic localization of functional mus-

carinic receptors in the rat superior cervical sympathetic ganglion reveals an extensive distribution over non-synaptic surfaces of neuronal somata, dendrites, and nerve endings. *Neuroscience* 71:797-832.

Risbo J, Jorgensen K, and others. 1997. Phase behaviour and permeability properties of phospholipid bilayers containing a short-chain phospholipid permeability enhancer. *Biochim Biophys Acta* 1329:85-96.

Roth A, Hausser M. 2001. Compartmental models of rat cerebellar Purkinje cells based on simultaneous somatic and dendritic patch-clamp recordings. *J Physiol (London)* 72: 445-472.

Santos-Sacchi J, Navarrete E. 2002. Voltage-dependent changes in specific membrane capacitance caused by prestin, the outer hair cell lateral membrane motor. *Pflugers Arch.* 444:99-106.

Schmid G, Goychuk I, and others. 2004. Gating charge effects on nerve excitation. Deutsche Physikalische Gesellschaft Conference, March 8-12, Regensburg, Germany.

Schwab A. 2001. Function and spatial distribution of ion channels and transporters in cell migration. *Am J Physiol Renal Physiol* 280:F739-47.

Siegel M, Marder E, and others. 1994. Activity-dependent current distributions in model neurons. *Proc Natl Acad Sci USA* 91:11308-11312.

- Stackgold I. 1979. *Greens Functions and Boundary Value Problems*. Wiley-Interscience, New York.
- Starr KA, Wolpaw JR. 1994. Synaptic terminal coverage of primate triceps surae motoneurons. *J Comp Neurology*, 345:345-358.
- Thurbon D, Luscher HR, and others. 1998. Passive electrical properties of ventral horn neurons in rat spinal cord slices. *J Neurophysiol* 80:2485-502.
- White JA, Manis PB, and others. 1992. The parameter identification problem for the somatic shunt model. *Biol Cyber* **66**:307-318.
- Williams SR, Stuart GJ. 2003. Voltage- and site-dependent control of the somatic impact of dendritic IPSPs. *J Neurosci*. 23:7358-7367.
- Wunch AD. 1994. *Complex Variables with Applications*, 2nd. Ed., Addison-Wesley, Boston.
- Zauderer E. 1983. *Partial Differential Equations of Applied Mathematics*. Wiley-Interscience, New York.

Tables

Table 1. Comparison of step change in membrane conductance with an exponential spatial variation in membrane conductance for a voltage response at $X=0$ to a current pulse stimulus at $X=0$ for a membrane cylinder with a length of $L = 1^a$. Amplitude coefficients are reported as a fraction of steady state. Z is the distance from the origin for a step change in membrane capacity (Fig. 1, inset).

Model	τ_0 (ms)	A_0	τ_1 (ms)	A_1
Exponential	4.822	0.7551	0.4334	0.1481
$Z = 0.2$	4.900	0.7543	0.4355	0.1465
$Z = 0.3$	4.850	0.7524	0.4304	0.1497
$Z = 0.4$	4.801	0.7515	0.4282	0.1522

^aThe first two Fourier coefficients were computed numerically using the eigenslope method (Knisley and Glenn 1997), and then verified using analytical expressions. The eigenvalues were found using a bisection method, and the slopes at the eigenvalues were found by the divided difference method (see Equation 4 in Section 7.1 of Kincaid and Cheney 1991). The τ_0 and τ_1 were computed for the point capacitance model with $C_s = 0.9 \mu F$, $C_m = 1 \mu F$, $R_m = 5,000 \Omega$, $L = 1$, and $\rho = 0.5, 1, 2, 3$.

Table 2. Comparison of point change in conductance (somatic shunt model) with an exponential spatial variation in membrane conductance (present model).

Model	τ_0 (ms)	τ_1 (ms)
Exponential	4.822	0.4333
Point, $\rho = .5$	4.701	1.0493
Point, $\rho = 1$	4.786	0.8738
Point, $\rho = 2$	4.863	0.7131
Point, $\rho = 3$	4.899	0.6396

Table 3. Eigenvalues and Fourier coefficients for decomposed experimental waveform (voltage responses to current step) and for model with exponentially-varying membrane conductance. Experimental data came from a spinal motoneuron from Glenn and others (1987). Amplitude coefficients are reported as a fraction of the steady state value, $V = 0.01266$.

	Experimental Data	Model Prediction
τ_0	5.28 ms	5.28 ms
τ_1	0.787 ms	0.866 ms
A_0	0.4779	0.4826
A_1	0.3791	0.2891

Table 4. Change in decay times in membrane cylinders with exponentially distributed non uniformity in C_m . The C_m was decreased across $[0,L]$ by 2% to 20%, decreased across $[0,L]$ from -2% to -20%, and made constant (0%). In all cases, the average C_m across $[0,L]$ remained constant (see 0%) at $R_m C_m = 0.01$ s. Other parameters: $L=1$, $I^{stim} = G^\infty$.

Percentage Increase in C_m	90% Decay Time (ms)	50% Decay Time (ms)	10% Decay Time (ms)
20%	0.12772	3.98	18.87
10%	0.14597	4.16	19.66
5%	0.15519	4.25	20.04
2%	0.15628	4.29	20.24
0%	0.15693	4.31	20.30
-2%	0.15774	4.33	20.51
-5%	0.15883	4.37	20.70
-10%	0.15948	4.41	21.06
-20%	0.15987	4.52	21.626

Figure Legends

Fig. 1. Dependence of decay time (τ) on electronic length (L) in the exponential model with a 10% origin-to-terminal capacitance change. Inset diagram summarizes the stimulation (I^{stim}) and response (V_m) points at $X=0$ and the longitudinal capacitance distribution in the point, step, and exponential models.

Fig. 2. A: Voltage response at the $X=0$ for the exponentially varying membrane capacity model. The parameters are R_m , C , C_m , L and G^∞ , where for each of the curves the membrane capacitance at $X=0$ (C) is indicated in the plot, and $C_m = 1.0 \mu\text{F}$, $R_m = 10^4 \Omega\text{-cm}$, $L=1$ and $G^\infty = I^{stim}$. **B:** Voltage response for the point model with the same parameters as in A.

Fig. 3. Experimental data (solid line) fit with a recording from the exponentially varying membrane capacity model (dashed line), from 1 ms to 10 ms.

Fig. 4. Effect of C_m non uniformity of 20% on passive voltage responses of a membrane cylinder. Average C_m over the cylinder was the same in all three models, but it decreased exponentially with distance in the upper curve (from 1.1 μF at $X=0$ to 0.9 at $X=L=1$), was constant in the middle curve, and increased exponentially with distance in the lower curve (from 0.9 μF at $X=0$ to 1.1 at $X=L=1$). Other parameters: $L=1$, $R_m = 10^4 \Omega\text{-cm}$, $I^{stim} = G^\infty$.

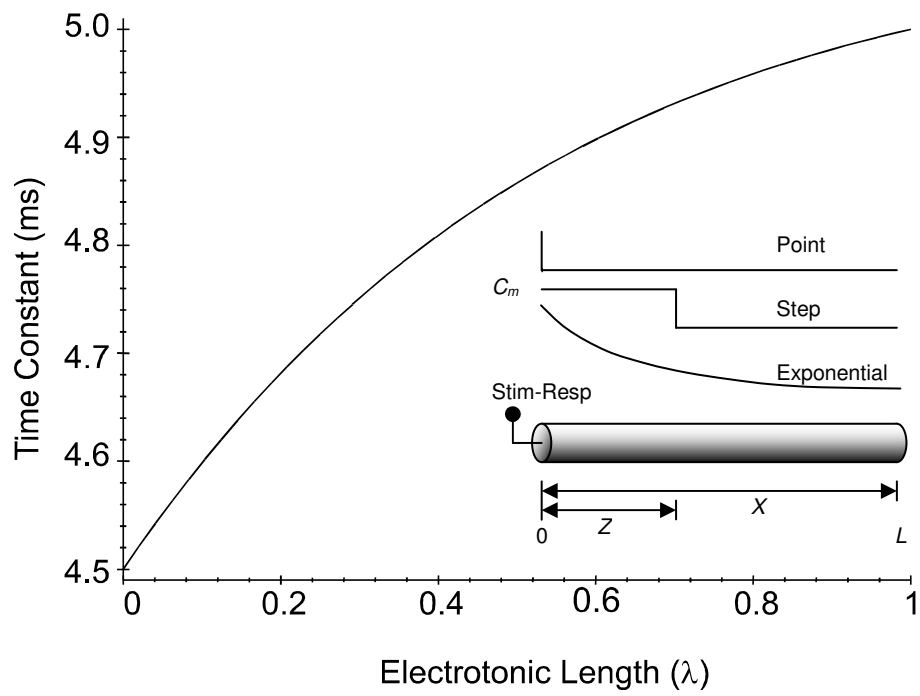


Fig. 1

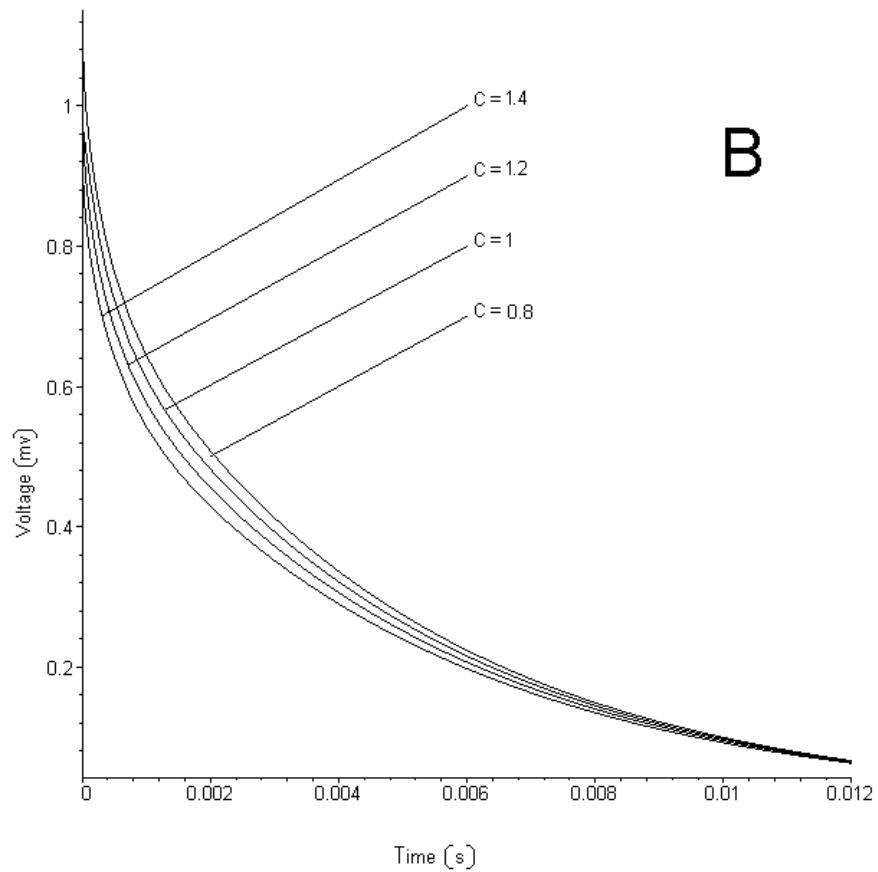
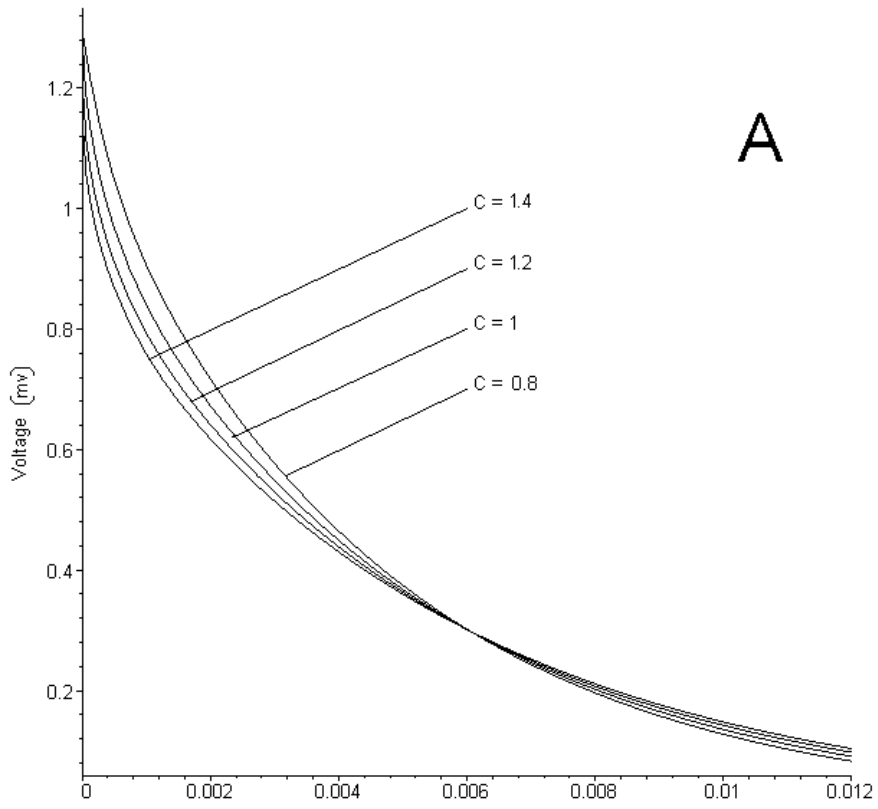


Fig. 2

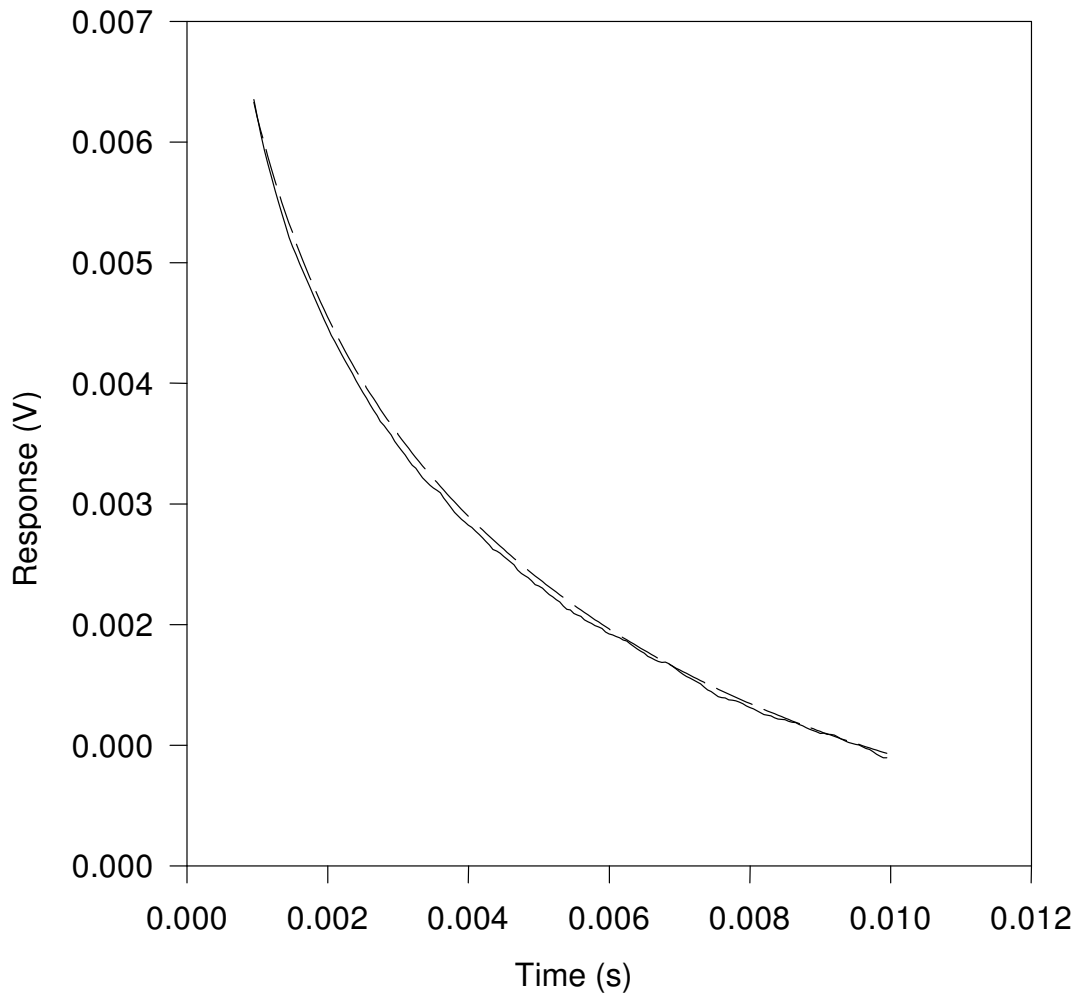


Fig. 3

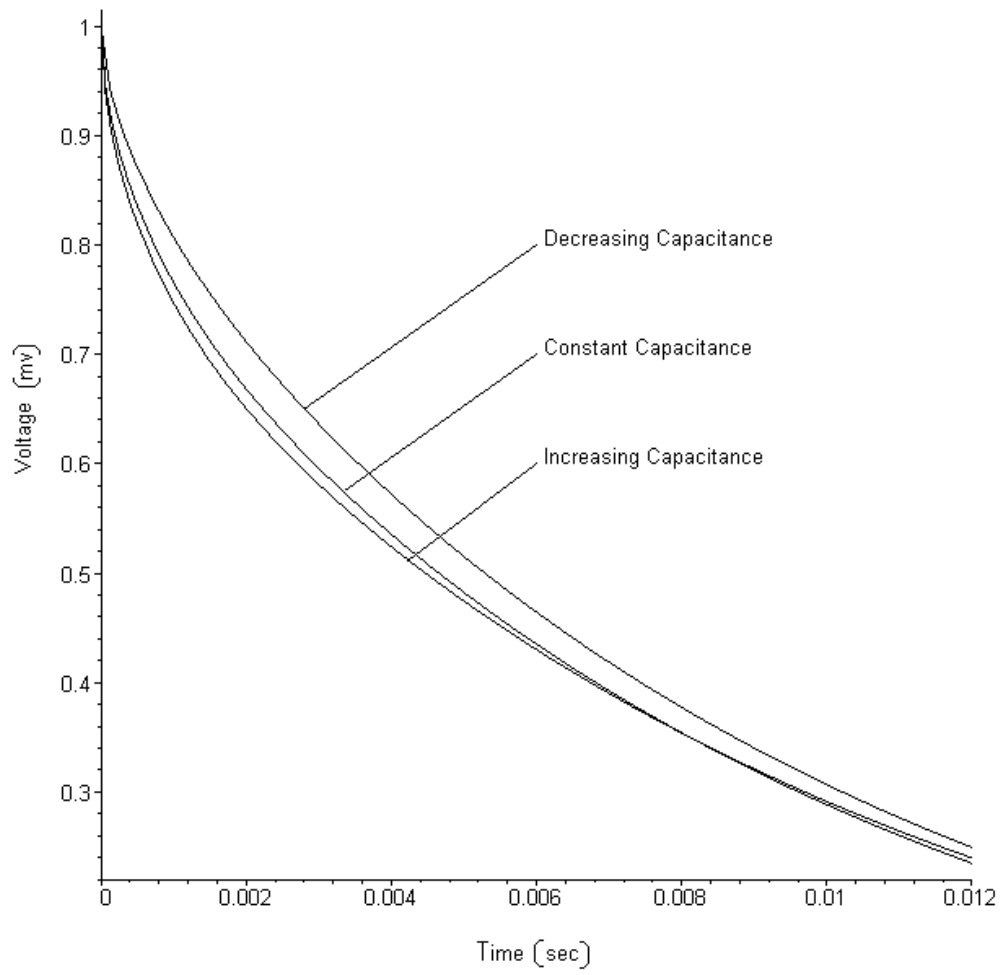


Fig. 4